Journal of Catalysis **190,** 338–351 (2000)
doi:10.1006/jcat.1999.2753, available online at http://www.idealibrary.com on IDEAL®

Dehydroisomerization of *n*-Butane over Pt–ZSM5

II. Kinetic and Thermodynamic Aspects

G. D. Pirngruber, K. Seshan, and J. A. Lercher[1]

Faculty of Chemical Technology, University of Twente, P.O. Box 217, 7500 AE Enschede, The Netherlands

Received July 29, 1999; revised November 1, 1999; accepted November 1, 1999

A kinetic model is applied to describe the dehydroisomerization of *n*-butane to isobutene over Pt–ZSM5. It is compared with experimental data and used to show how a combination of kinetics and thermodynamics affects the obtained yields. High temperatures reduced the selectivity to by-product formation by oligomerization/cracking of butenes. However, the stability of the catalyst decreased. This is attributed to the enhanced formation of butadiene, poisoning metal and acid sites. Lowering the pressure also reduced the selectivity to by-products and the thermodynamic constraints and was, thus, favorable for dehydroisomerization. The H_2/*n*-butane ratio mainly affected the selectivity to hydrogenolysis, which increased with hydrogen partial pressure, while catalyst stability did not improve significantly. An optimum with respect to selectivity and stability was found for a H_2/*n*-butane ratio of 2.

Key Words: **dehydroisomerization; bifunctional catalysis; Pt–ZSM5; kinetic modeling.**

INTRODUCTION

Isobutene is an important intermediate in the petrochemical industry. Its production is usually integrated in refinery processes leading to MTBE or alkylate (1) as a final product. Pure isobutene is used for the synthesis of polymers, such as butyl rubber, polybutene, and isoprene (2).

Since there is an abundant supply of butanes from natural gas reserves and refinery streams, butanes are the preferred raw material for the production of isobutene. The synthesis of isobutene from butane is usually done in a two-step process, comprising an isomerization, a separation, and a dehydrogenation unit (3–5). A direct, one-step synthesis poses a conceptually interesting alternative. In a recent publication we reported that Pt–ZSM5 can be successfully used as a catalyst for such a direct conversion of *n*-butane to isobutene (6).

The previous paper addressed mainly the reaction network and the influences of the catalyst parameters, metal loading, and acid site concentration. It was found that high metal loadings and low acid site concentrations were important to obtain an active and selective dehydroisomerization catalyst. The present study focuses on the optimization of reaction parameters, such as pressure, temperature, etc., with the aim to quantify the reaction kinetics and to achieve a further improvement in the yield and selectivity of isobutene.

It had been concluded (6) that secondary cracking of butenes (via formation of di- and oligomers) was the major source of by-products in the dehydroisomerization of *n*-butane over Pt–ZSM5. Oligomerization/cracking of butenes is favored at low temperatures and high pressures (7). Thus, higher selectivities to isobutene can be expected when the dehydroisomerization of *n*-butane is carried out at higher temperatures and lower pressures. Moreover, higher temperatures and lower pressures increase the thermodynamically possible yields of *n*-butenes and of isobutene. In order to experimentally establish these effects, the influence of pressure and temperature on the dehydroisomerization of *n*-butane was studied.

In addition to pressure and temperature, the hydrogen-to-hydrocarbon ratio is an important parameter of the reaction. Hydrogen is added to the feed in order to maintain the stability of the catalyst. From a thermodynamic point of view, addition of hydrogen is not desirable, since it shifts the dehydrogenation equilibrium to the side of the reactant. In addition, hydrogenolysis reactions could possibly be reduced if the hydrogen concentration in the reaction mixture was minimized. A priori it is not possible to predict which of these effects dominates in importance. The role of the hydrogen-to-hydrocarbon ratio with respect to catalyst stability, activity, and selectivity to by-products was, therefore, explored.

EXPERIMENTAL

For studying the effects of temperature, pressure, and hydrogen/*n*-butane ratio, two materials were chosen, 0.1% Pt–ZSM5 ($SiO_2/Al_2O_3 = 480$) and 0.5% Pt–ZSM5

[1] Present address: Institute for Chemical Technology, Technische Universität München, Lichtenbergstr. 4, D-85748 Garching, Germany.

0021-9517/00 $35.00

($SiO_2/Al_2O_3 = 480$) (see Ref. 6). They were prepared by slow addition of a diluted solution of $Pt(NH_3)_4(OH)_2$ (0.1–0.2 mg of Pt/l) and ammonia (~2 vol%) to a suspension of the parent zeolite (CBV 10002, from ZEOLYST Int.) in water (10 ml of H_2O/g of zeolite), followed by stirring for 12 h. After filtering and drying, the zeolite was slowly heated (0.5 K/min) in a flow of dry air to 723 K and kept there for 2 h. The catalyst was cooled to 400 K and flushed with dry nitrogen. Subsequently, the sample was reduced in a flow of H_2 (~250 cm^3/min STP), ramping the temperature to 773 K at 5 K/min and remaining at 773 K for 2 h.

ZSM5 samples ($SiO_2/Al_2O_3 = 215$) with different crystal sizes (1 and 4 μm) were received from Exxon. The 0.5% Pt was incorporated by the method described above.

The elemental composition of the samples was determined by X-ray fluorescence. Hydrogen chemisorption for determining the Pt dispersion was carried out in a volumetric system. About 1 g of the sample was reduced for 1 h at 823 K in H_2. After reduction, the sample was degassed at 823 K (which was also the reaction temperature) for 1 h in vacuum (10^{-5} mbar). After degassing, the sample was cooled to room temperature and the hydrogen adsorption isotherm was measured by dosing decreasing amounts of H_2 (in the range of 500 to 50 mbar) to the sample. The hydrogen chemisorption capacity was calculated by extrapolation of the hydrogen uptake to zero pressure (8). The concentration of Brønsted acid sites was determined from the intensity of the band at 3610 cm^{-1} in the IR spectrum of the sample, attributed to the stretching vibration of the Brønsted OH groups. Details of the experimental procedures are given in Ref. (6). The results of the characterization are summarized in Table 1.

For the catalytic tests the samples were pressed, crushed, and sieved to obtain a particle size in the range of 300 to 500 μm. From 10 to 50 mg of the catalyst was mixed with 50 to 100 mg of quartz and filled into a quartz tube with an inner diameter of 4 mm. The catalyst bed had a typical length of 5 to 15 mm and was supported on both sides by quartz wool.

The samples were reduced *in situ* at 830 K for at least 1 h in a mixture of H_2/Ar (18/82), and then cooled to reaction temperature. The reaction was started by switching from H_2/Ar to the feed, which was under standard conditions a mixture of 10% *n*-butane, 20% H_2, the balance being Ar. Yields of products and the conversion of *n*-butane were reported on the basis of moles of carbon converted. The reproducibility of the product yields and the *n*-butane conversion was about ±15% for the initial values (at zero time on stream) and about ±5% for the steady-state values. Due to the lower catalyst mass used, the largest error margins were observed for experiments performed at high weight hourly space velocities (WHSVs).

Since dehydrogenation and isomerization are close to equilibrium at higher conversions, equilibrium effects significantly influence the measured reaction rates. Therefore, the catalytic activity was expressed in terms of pseudo-first-order rate constants, which were calculated from a kinetic model assuming first order in the forward and backward reaction steps (see Appendix 1 for the details of the calculation). While this model has a limited accuracy in describing the real kinetics, it helped to reduce the dependence of the reaction rates on the level of conversion, thereby facilitating the evaluation of rate constants.

TABLE 1

Physico-chemical Characterization of the Pt–ZSM5 Samples

Sample code	SiO_2/Al_2O_3	H^+ (mmol/g)	Pt loading (wt%)	H/Pt
0.1% Pt–ZSM5(480)	480	0.07	0.09	>2.0
0.5% Pt–ZSM5(480)	480	0.07	0.46	1.2
0.5% Pt–ZSM5(1 μm)	215	0.15	0.51	1.5
0.5% Pt–ZSM5(4 μm)	215	0.15	0.53	1.5

RESULTS

Effect of Temperature

Figure 1 shows the effect of temperature on the activity of 0.1 and 0.5% Pt–ZSM5(480). The initial conversion increased with temperature. On the other hand, the catalyst deactivated faster at higher temperatures. We calculated the activation energy of dehydrogenation from the initial rates of butene formation, at a constant conversion level of 15%. This was the lowest conversion at which a comparison of all catalysts and temperatures was possible. Values of 50 and 85 kJ/mol were obtained for 0.1 and 0.5% Pt–ZSM5(480), respectively. At 15% conversion, however, equilibrium effects already play a role. In order to correct for these effects, the activation energy was determined from the temperature dependence of the rate constant of dehydrogenation (k_1), which was calculated from the initial conversions,[2] using the method described in Appendix 1. Figure 2 shows the respective Arrhenius plots for both catalysts. The corrected activation energies were 25 and 40 kJ/mol for 0.1 and 0.5% Pt–ZSM5(480), respectively. The scatter of the data was very large, however, and the error margin of the activation energy was estimated to be 10 kJ/mol. The stronger temperature dependence of 0.5% Pt–ZSM5(480) was, however, significant. It was also reflected in the steady-state yield of the sum of butenes ($\sum C_4^=$) achieved at higher space times. From 775 to 830 K it increased by a factor of 2 for 0.5% Pt–ZSM5(480), but only

[2] A small increase of the conversion, which was sometimes observed in the first minutes on stream, was attributed to transient phenomena and not taken into account in the extrapolation of the initial conversion.

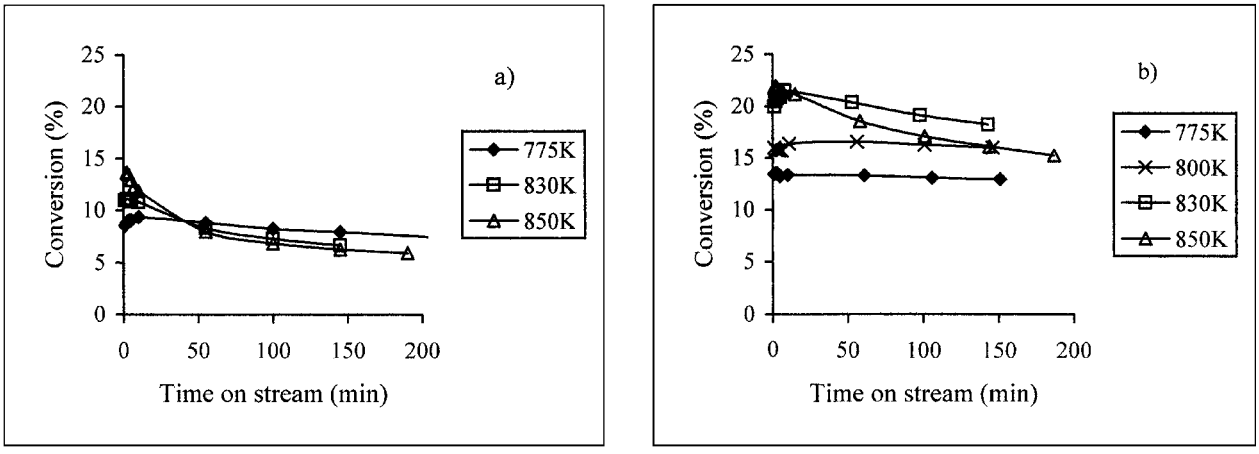

FIG. 1. Conversion of *n*-butane as a function of temperature. Conditions: WHSV = 260 h^{-1}, 1.8 bar, 10% *n*-butane, 20% H_2. (a) 0.1% Pt–ZSM5(480), (b) 0.5% Pt–ZSM5(480).

by a factor of 1.5 for 0.1% Pt–ZSM5(480) (see Table 2). The effect of temperature on the selectivities is shown in Table 3. As expected, the selectivity to secondary cracking (i.e., to oligomerization/cracking of the butenes) decreased with temperature, while the selectivity to dehydrogenation increased. Moreover, the selectivity to isobutane decreased drastically from 775 to 830 K.

Effect of Pressure

Table 4 shows the conversion, the rate of dehydrogenation, and the calculated pseudo-first-order rate constant of dehydrogenation as a function of pressure. (The lower pressure limit was given by the pressure drop at high flow rates.) The conversion and the rate of dehydrogenation were practically independent of pressure at 775 K and increased slightly at 830 K. As already mentioned above, a comparison of the reaction rates may be misleading because of the pressure dependence of the dehydrogenation equilibrium. Therefore, also the pseudo-first-order rate constants k_1 of dehydrogenation are given in Table 4. They decreased with increasing pressure.

For practical applications, the effect of pressure at high conversions is more relevant than the variations at low conversions. Table 5 compiles some activity data at WHSV = 20 h^{-1}. In the case of 0.1% Pt–ZSM5(480), pressure had only a minor effect on the steady-state activity. In the case of 0.5% Pt–ZSM5(480), however, a *higher* conversion of *n*-butane and a higher yield of butenes were obtained at a *lower* pressure. With respect to the selectivity, reducing the pressure from 1.8 to 1.0 bar caused the expected increase in selectivity to dehydrogenation and a decrease in selectivity to secondary cracking. The selectivity to isobutane also decreased drastically.

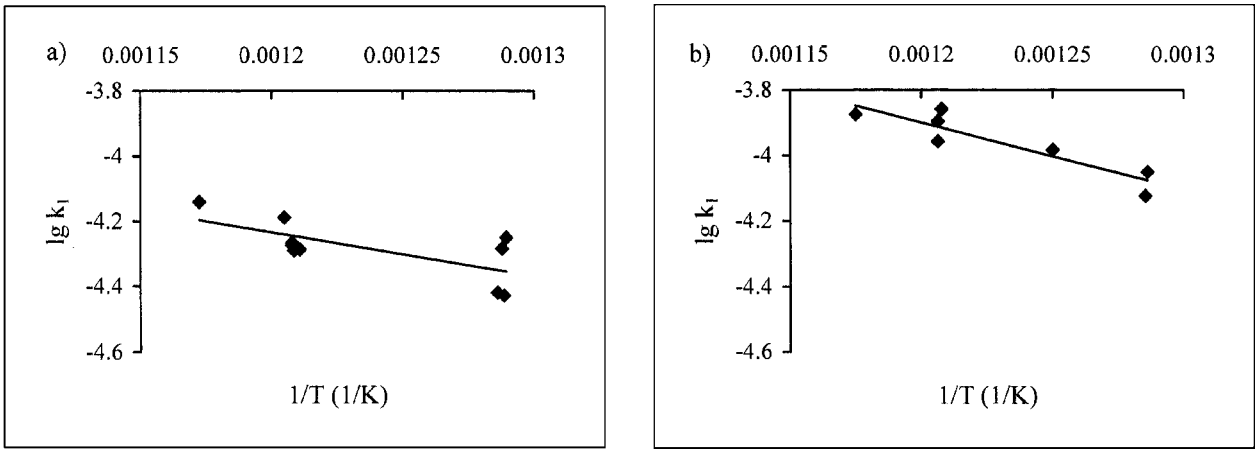

FIG. 2. Arrhenius plot of the pseudo-first-order rate constant of dehydrogenation (k_1). k_1 was calculated by the method described in Appendix 2, using the initial conversion of *n*-butane (at zero time on stream). (a) 0.1% Pt–ZSM5(480), (b) 0.5% Pt–ZSM5(480).

TABLE 2

Steady-State Yields and Conversions at a Constant WHSV = 20 h^{-1} (ST = 30,000 s g/m^3)

	0.1% Pt–ZSM5(480)		0.5% Pt–ZSM5(480)	
	775 K	830 K	775 K	830 K
Yield i-$C_4^=$	5.1	8.1	5.0	12.1
Yield $C_4^=$	18.2	25.8	19.1	37.5
Conversion	22.6	30.6	31.0	52.9
i-$C_4^=/\sum C_4^=$	28.1	31.4	25.9	32.2

Conditions: 1.8 bar, 10% *n*-butane, 20% H_2, 100 min time on stream. Yields and conversion in mol% carbon.

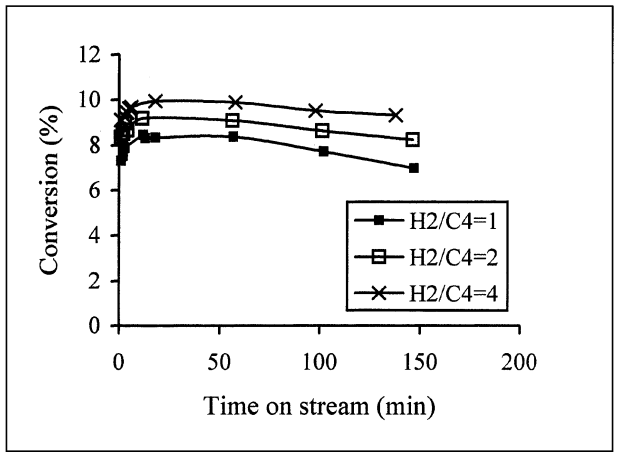

FIG. 3. Conversion of *n*-butane as a function of H_2/*n*-butane ratio. Conditions: WHSV = 170 h^{-1}, 775 K, 1.25 bar, 10% *n*-butane, 20% H_2, 0.1% Pt–ZSM5(480).

Effect of Hydrogen/Hydrocarbon Ratio

Figure 3 shows the conversion of *n*-butane as a function of time on stream for three different H_2/*n*-butane ratios (WHSV = 170 h^{-1}). For the H_2/*n*-butane ratios of 3.6, 2.0, and 1.1, deactivation rates $-dk_1/dt$ of $(1.0 \pm 0.4) \times 10^{-9}$, 1.0×10^{-9}, and $(1.3 \pm 0.1) \times 10^{-9}$ $m^3\,s^{-2}\,g^{-1}$ were calculated (from the decrease of activity between 50 and 150 min time on stream). Thus, the deactivation rate decreased only marginally with increasing H_2/*n*-butane ratio.

The H_2/*n*-butane ratio also had a non-negligible effect on the conversion. It increased with hydrogen partial pressure. A plot of $\ln(k_1)$ vs $\ln(p_{H_2})$ yielded an order of approximately 0.4 in hydrogen. At higher contact times, however, the H_2/*n*-butane ratio had only a minor effect on the steady-state conversion of *n*-butane (see Table 6). A small optimum in the yield of the sum of butenes and of isobutene was observed for H_2/*n*-butane = 2.

An analysis of the by-product pattern showed that higher H_2/*n*-butane ratios led to an increase in selectivity to methane, ethane (see Fig. 4), and isobutane. Also the rates of methane and ethane formation increased with hydrogen partial pressure (see Fig. 5). The intercept of both curves was zero, indicating that the presence of hydrogen is necessary for the formation of these products. Assuming a power rate law $r = r_0 p_{H_2}^x$, an order of 1 and 1.6 in hydrogen was obtained for methane and ethane, respectively.

TABLE 3

Effect of Temperature on the Steady-State Selectivities (in mol% Carbon)

	0.1% Pt–ZSM5(480), conversion = 22.5%		0.5% Pt–ZSM5(480), conversion = 31%	
	775 K	830 K	775 K	830 K
CH_4	0.7	0.6	3.2	1.7
i-C_4	5.9	0.9	13.0	2.0
i-$C_4^=$	22.6	22.6	16.0	19.0
$C_4^=$	80.4	91.1	61.6	82.0
Sec. cracking[a]	10.8	5.3	20.1	12.0

Conditions: 1.8 bar, 10% *n*-butane, 20% H_2, 100 min time on stream.
[a] Counted as the sum of ethane, propane, propene, and pentene (see Ref. 6).

Diffusional Constraints

In order to probe the presence of external diffusion limitations, the flow rate was varied while the space time was kept constant (9). The difference between these experiments was within the error of measurement (<10% for the initial conversion, <2% for the steady-state conversion). In order to check the effect of intraparticle diffusion (i.e., within the 300–500-μm particles that were pressed from the zeolite powder) also a smaller sieve fraction of 100–300-μm particles was tested. The smaller particles tended to give higher conversions (the difference was 0 to 20% for the initial conversion and 0 to 10% for the steady-state conversion). The small increase was rather attributed to the higher pressure drop that was observed with the small particles than to the presence of intraparticle diffusion limitations.

Finally, in order to establish the influence of micropore diffusion (intracrystalline diffusion), the dehydroisomerization of *n*-butane was performed over 0.5% Pt–ZSM5 catalysts with different crystal sizes (1 and 4 μm). Figure 6 shows the respective results. Only marginal differences were observed. The conversion and the yield of the sum of butenes increased slightly with crystal size, while the ratio of isobutene to the sum of butenes decreased slightly.

As a control experiment, butene isomerization was performed over the parent ZSM5 materials (without Pt). Also here, an influence of crystal size on the yield of isobutene was not observed.

TABLE 4

Conversion of *n*-Butane, Rate of Dehydrogenation ($\sum C_4^=$), and Pseudo-First-Order Rate Constant of Dehydrogenation (k_1), Calculated from the Initial Conversion

	0.1% Pt–ZSM5(480)			0.5% Pt–ZSM5(480)		
	Conv (%)	Rate (10^{-5} mol/s g)	k_1 (10^{-5} m^3/s g)	Conv (%)	Rate (10^{-5} mol/s g)	k_1 (10^{-5} m^3/s g)
			775 K, WHSV = 170 h^{-1}			
1.25 bar	9.2	7.2	4.5	15.5	12	9.4
1.8 bar	9.7	7.7	3.8	14.8	12	7.5
			830 K, WHSV = 260 h^{-1}			
1.4 bar	8.8	11	6.1	17.9	21	16.8
1.8 bar	11.0	12	5.3	21.5	24	12.8

Feed: 10% *n*-butane, 20% H_2.

DISCUSSION

Kinetic Model of Dehydroisomerization

Dehydroisomerization can be described as sequence of two reversible reactions.

$$n\text{-}C_4H_{10} \rightleftharpoons n\text{-}C_4H_8 \rightleftharpoons \text{i-}C_4H_8$$

Assuming first-order rate equations the kinetics is described by

$$\frac{d[n\text{-}C_4H_{10}]}{dt} = -k_1[n\text{-}C_4H_{10}] + k_{-1}[n\text{-}C_4H_8] \quad [1]$$

$$\frac{d[n\text{-}C_4H_8]}{dt} = -\frac{d[n\text{-}C_4H_{10}]}{dt} - \frac{d[\text{i-}C_4H_8]}{dt} \quad [2]$$

$$\frac{d[\text{i-}C_4H_8]}{dt} = k_2[n\text{-}C_4H_8] - k_{-2}[\text{i-}C_4H_8] \quad [3]$$

k_1 and k_{-1} are the forward and backward rate constants of dehydrogenation. k_2 and k_{-2} are the forward and backward rate constants of butene isomerization. k_1 and k_{-1} and k_2 and k_{-2} are related to each other by the equilibrium constants of dehydrogenation[3] and isomerization (K_1 and K_2), respectively.

$$K_1 = [n\text{-}C_4H_8]_{eq}/[n\text{-}C_4H_{10}]_{eq} = k_1/k_{-1} \quad [4]$$

$$K_2 = [\text{i-}C_4H_8]_{eq}/[n\text{-}C_4H_8]_{eq} = k_2/k_{-2} \quad [5]$$

The analytical solution of the equation system [1]–[3] is described by Rodiguin and Rodiguina (10). It was compared with the presented experimental data. The 0.1% Pt–ZSM5(480) was used, since a large amount of experimental data was available for this catalyst. k_1 was estimated from rate data at low conversions (see Table 4). k_2 was determined by measuring the rate of butene isomerization over ZSM5(480). K_1 and K_2 were calculated from thermodynamic data (11). Figure 7 compares the model calculation with the experimental data. Two main differences were observed. (i) At higher space times the conversion decreased faster than predicted by the model. Obviously, factors which retard the reaction at higher conversions were not taken into account in the simple first-order kinetics. (ii) The model underestimates the ratio i-$C_4^=/(\sum C_4^=)$ when the experimentally determined rate constant of butene isomerization is used as k_2.

In order to get a better description of the experimental data a more detailed kinetic model was developed. The following sequence of elementary steps was assumed (12–16) (*M* represents an adsorption site on the metal).

$$2M + n\text{-}C_4H_{10}(g) \rightleftharpoons M\text{–}C_4H_9 + M\text{–}H \quad [i]$$

$$M\text{–}C_4H_9 + 2M \rightleftharpoons M_2\text{–}C_4H_8 + M\text{–}H \quad [ii]$$

$$M_2\text{–}C_4H_8 \rightleftharpoons 2M + n\text{-}C_4H_8(g) \quad [iii]$$

$$2M\text{–}H \rightleftharpoons 2M + H_2(g) \quad [iv]$$

TABLE 5

Effect of Pressure on the Activity

	0.1% Pt–ZSM5(480)		0.5% Pt–ZSM5(480)	
	1.0 bar[a]	1.8 bar	1.0 bar[a]	1.8 bar
Yield i-$C_4^=$ (%)	5.0	5.1	5.4	5.0
Yield $C_4^=$	20	18.2	27	19.1
Conversion (%)	22	22.6	35	31.0
i-$C_4^=/C_4^=$ (%)	25	28.1	25	25.9

Conditions: WHSV = 20 h^{-1}. 100 min time on stream, 775 K, 10% *n*-butane, 20% H_2. Yields and conversion in mol% carbon.

[a] Values were interpolated.

[3] The small variation of $[H_2]$ in the course of the reaction was neglected ($[H_2]$ does not vary more than 10% from its feed level, see Ref. 6) and $[H_2]$ included in the value of K_1.

TABLE 6

Conversion of *n*-Butane and Yield of the Sum of Butenes and of Isobutene

	H_2/*n*-butane		
	1.1	2.0	3.6
Yield i-$C_4^=$	5.9	6.5	5.8
Yield $C_4^=$	21.0	23.1	20.3
Conversion	23.6	26.3	25.4
i-$C_4^=$/$C_4^=$	27.8	28.3	28.5

Conditions: WHSV = 12 h^{-1}, 775 K, 1.0 bar, 10% *n*-butane. 0.1% Pt–ZSM5(480).

Also the formation of butadiene via more highly dehydrogenated surface species was included in the model.

$$M_2\text{–}C_4H_8 + 4M \rightleftharpoons M_4\text{–}C_4H_6 + 2M\text{–}H \qquad [v]$$

$$M_4\text{–}C_4H_6 \rightleftharpoons C_4H_6 + 4M \qquad [vi]$$

Hydrogen/deuterium exchange experiments (15, 17) suggested that step [i], the dissociative abstraction of the first hydrogen, is rate determining. Steps [ii]–[vi] can then be assumed to be in quasi-equilibrium, which yields the following equations for the rates and surface coverages.

$$\begin{aligned} r &= \kappa_1\Theta_*^2[n\text{-}C_4H_{10}] - \kappa_{-1}\Theta_{C_4H_9}\Theta_H \\ \kappa_2\Theta_{C_4H_9}\Theta_*^2 &= \kappa_{-2}\Theta_{C_4H_8}\Theta_H \\ \kappa_3\Theta_{C_4H_8} &= \kappa_{-3}\Theta_*^2[n\text{-}C_4H_8] \\ \kappa_4\Theta_H^2 &= \kappa_{-4}\Theta_*^2[H_2] \\ \kappa_5\Theta_{C_4H_8}\Theta_*^4 &= \kappa_{-5}\Theta_{C_4H_6}\Theta_H^2 \\ \kappa_6\Theta_{C_4H_6} &= \kappa_{-6}[C_4H_6]\Theta_*^4 \end{aligned} \qquad [6]$$

Θ_* represents the free fraction of the metal surface, Θ_H the fraction of Pt covered by H, $\Theta_{C_4H_9}$ the fraction covered by C_4H_9, $\Theta_{C_4H_8}$ the fraction covered by the olefin precursor

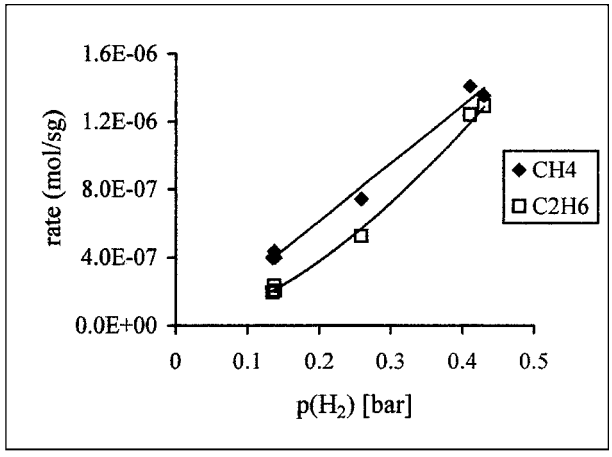

FIG. 5. Rate of methane and ethane formation as a function of hydrogen partial pressure. Conversion, 8–10%. Conditions: WHSV = 170 h^{-1}, 775 K, 1.25 bar, 10% *n*-butane, 20% H_2, 100 min time on stream, 0.1% Pt–ZSM5(480).

C_4H_8, etc. IR studies (at temperatures below 300 K) indicated that butenes are adsorbed on Pt as π-bonded species, di-σ-bonded species, and tri-σ-bonded alkylidyne species (18, 19), the latter two prevailing at higher temperatures (19). Natal-Santiago *et al.* have suggested the presence of even more highly dehydrogenated species in the adsorption of isobutene on Pt (1,1,1,2-tetra-σ and 1,1,1,3-tetra-σ) (20). For the sake of simplicity we assumed the olefin to be adsorbed as a di-σ species, i.e., occupying two Pt sites, while all more highly dehydrogenated species are tetra-σ-adsorbed and lead to the formation of butadiene. The above set of equations [6] gives the following expression for the reaction rate (15, 16).

$$r = \kappa_1\Theta_*^2[C_4H_{10}]\left[1 - \frac{1}{K_{eq}}\frac{[n\text{-}C_4H_8][H_2]}{[n\text{-}C_4H_{10}]}\right] \qquad [7]$$

K_{eq} is the equilibrium constant of the overall reaction.

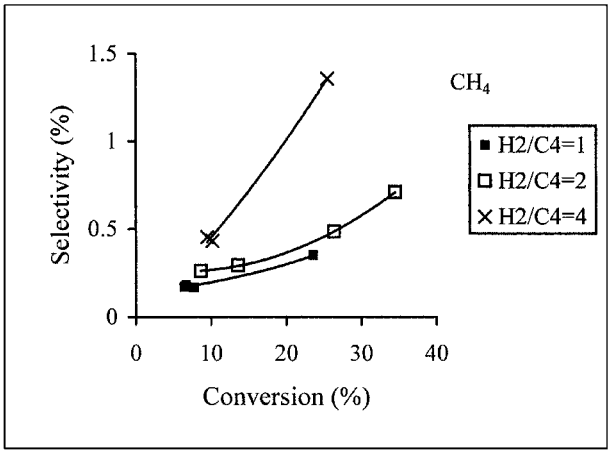

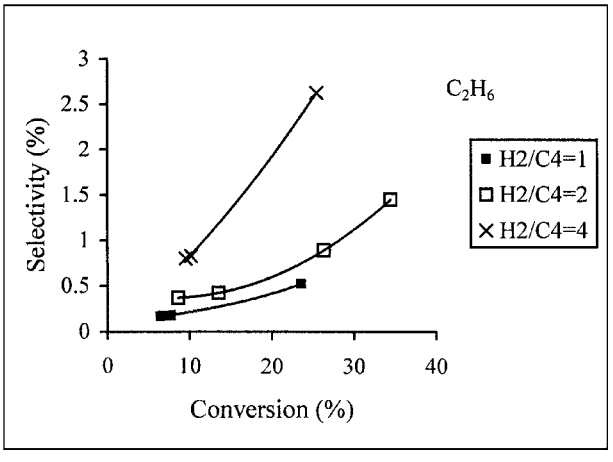

FIG. 4. Selectivity to methane and ethane as a function of H_2/*n*-butane ratio. Conditions: 775 K, 1.0 bar, 10% *n*-butane, 20% H_2, 100 min time on stream, 0.1% Pt–ZSM5(480).

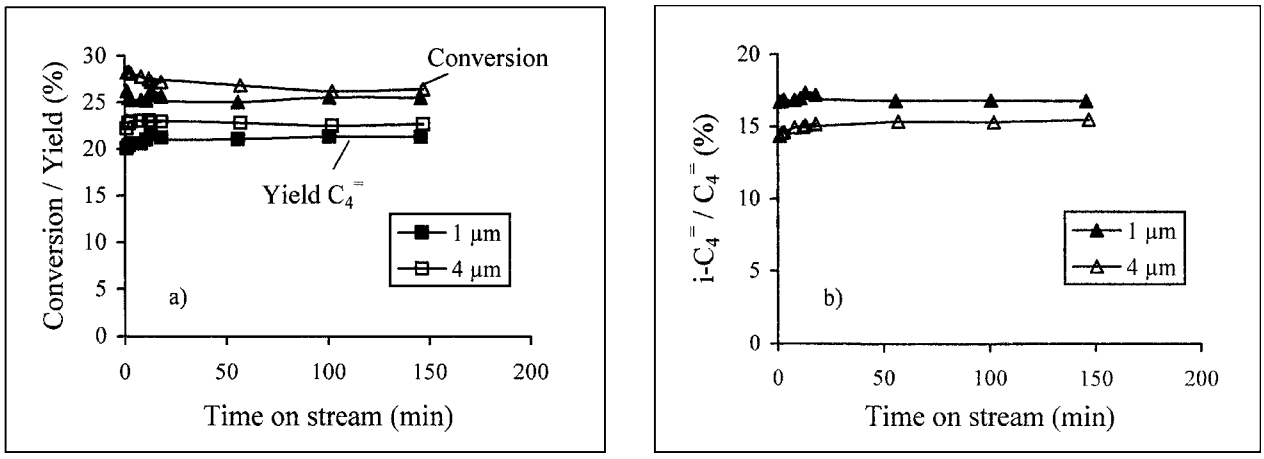

FIG. 6. Dehydroisomerization of *n*-butane over 0.5% Pt–ZSM5(215) with crystal sizes of 1 (solid symbols) and 4 μm (open symbols). (a) Conversion of *n*-butane and yield of the sum of butenes. (b) Ratio i-$C_4^=/\sum C_4^=$. Conditions: WHSV = 170 h^{-1}, 775 K, 1.2 bar, 10% *n*-butane, 20% H_2.

The fraction of free sites (Θ_*) can be calculated from the sitebalance $\Theta_* + \Theta_{C_4H_9} + 2\Theta_{C_4H_8} + 4\Theta_{C_4H_6} + \Theta_H = 1$. By a detailed kinetic analysis of isobutane dehydrogenation on Pt/Sn–SiO_2, Cortright *et al.* showed that the fractional coverage of the butyl species (C_4H_9) is very low (less than 10^{-5}) (15). Thus, $\Theta_{C_4H_9}$ is neglected for the sake of simplifying the expression. Likewise, the adsorption of hydrogen is weak compared to the adsorption of the alkene. In microcalorimetric studies an initial heat of sorption of more than 200 kJ/mol was measured for the adsorption of isobutene on Pt–SiO_2 (20) and for *cis*-2-butene on Pt–NaY (21), compared to only 100 kJ/mol for hydrogen. Our own experiments showed a positive order in hydrogen, while a negative order would be expected if the surface coverage of hydrogen was high. Thus, we concluded that M_2–C_4H_8 and M_4–C_4H_6 were the dominating surface species, while Θ_H was low[4]. With these assumptions the site balance reduced to

$$4\Theta_{C_4H_6} + 2\Theta_{C_4H_8} + \Theta_* = 4K_{C_4H_6}[C_4H_6]\Theta_*^4 + 2K_{C_4H_8}[C_4H_8]\Theta_*^2 + \Theta_* = 1, \quad [8]$$

where $K_{C_4H_8} = \kappa_3/\kappa_3$ is the adsorption constant of *n*-butene on the metal and $K_{C_4H_6} = \kappa_6/\kappa_6$ is the adsorption constant of butadiene on the metal. Note that since steps [iii] to [vi] were assumed to be in quasi-equilibrium, the concentrations of butene and butadiene are tied to each other by

$$[C_4H_6] = \frac{K_5 K_{C_4H_8}}{K_{H_2} K_{C_4H_6}} \frac{[C_4H_8]}{[H_2]}, \quad [9]$$

where K_5 is the equilibrium constant of step [v] and K_{H_2} the adsorption constant of H_2. This is in agreement with the experimental observation that a constant ratio of butadiene to the sum of butenes was found for a certain set of reaction conditions.

Equation [8] was numerically solved and the solution substituted in Eq. [7]. For describing the dehydroisomerization reaction, Eq. [7] was combined with Eqs. [2] and [3]. Note that at low coverages ($\Theta_* \sim 1$) Eq. [7] reduces to Eq. [1]. Under these conditions the refined model and the original model are equivalent. Readsorption of isobutene on the metal was accounted for by using the sum of all butenes in the term $[C_4H_8]$ in Eq. [8] instead of only the linear butenes.

With $k_1 = 5 \times 10^{-5}$ $m^3/s\,g$, $k_2 = 8 \times 10^{-5}$ $m^3/s\,g$, $RTK_{C_4H_8} = 10$ bar^{-1}, $RTK_{C_4H_6} = 400$ bar^{-1}, and $[C_4H_6]/[C_4H_8] = 0.027$ (the average ratio found in the experiments) a good fit of the experimental values was obtained (see Fig. 8). k_2 had to be chosen higher than 4.5×10^{-5} m^3/s g (experimentally measured for butene isomerization) in order to obtain a good fit of the isomer fraction at low space times. At high space times the model overestimated the isomer fraction. This is due to an increasing contribution of oligomerization/cracking reactions, which were not taken into account in the model. A more detailed discussion of the choice of the model parameters is given in Appendix 2.

The Effect of Temperature and Pressure

The effect of temperature and pressure on the dehydroisomerization reaction is threefold: (i) on the selectivity to by-products, especially oligomerization/cracking of butenes, (ii) on the thermodynamic constraints, and (iii) on

[4] Note that most kinetic studies, in which negative orders in hydrogen were found, were performed at low conversions and high hydrogen partial pressures. Under these conditions hydrogen is the dominating surface species despite its lower heat of sorption. At high conversions and low H_2/hydrocarbon ratios, however, the coverage changes in favor of the alkene, as confirmed by calculations, using the above-mentioned heats of sorption and thermodynamic data for the sorbed state given in Ref. (16).

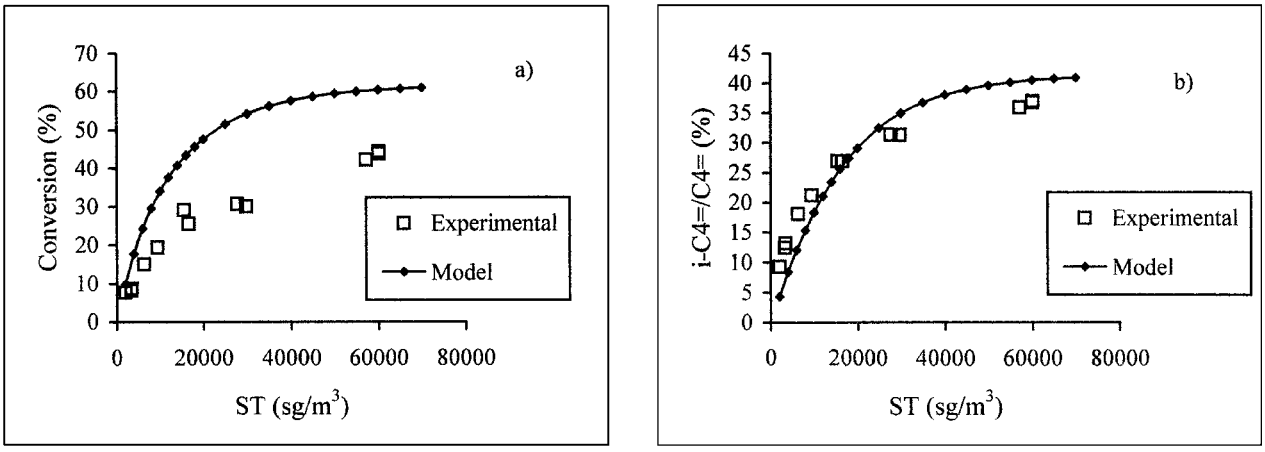

FIG. 7. Comparison of experimental data with a first-order kinetic model. Experimental data: 0.1% Pt–ZSM5(480), 830 K, 1.8 bar, 10% *n*-butane, 20% H_2, 100 min on stream. Model parameters: $k_1 = 5.5 \times 10^{-5}$ m^3/s g, $k_2 = 4.5 \times 10^{-5}$ m^3/s g, $K_1 = 0.94$, $K_2 = 0.71$.

the kinetics. With respect to selectivity, the catalysts showed the expected trend. The contribution of butene oligomerization/cracking decreased with increasing temperature and decreasing pressure, as predicted in Ref. (7). Thus, we focus the discussion on the interaction between thermodynamic constraints and kinetics.

Figure 9 shows how the thermodynamically possible yields of isobutene and the sum of butenes change with temperature and pressure. The maximum yield of isobutene (keeping the pressure constant at 1.8 bar) can be obtained at 900 K. But thermodynamics also predicts a sharp increase in butadiene formation above 830 K. This is not desirable, since butadiene is known to cause catalyst deactivation (13).

The thermodynamically predicted increase in butadiene formation with temperature was experimentally confirmed (see Table 7). In parallel, the deactivation rates of both reaction steps, dehydrogenation and isomerization, increased. This suggests that the enhanced butadiene formation is in fact responsible for the poisoning of metal and acid sites at high temperatures.

The experimental results suggest that 830 K is a good compromise with respect to the reaction temperature. While thermodynamic and selectivity aspects would advise the use of even higher temperatures, the actual steady-state conversions are not improved by raising the temperature above 830 K (see Fig. 1), because catalysts deactivate faster at higher temperatures.

In order to discuss the effect of pressure on the kinetics and thermodynamics of dehydroisomerization on Pt–ZSM5, we used the kinetic model described in the previous section. Figure 10 compares the calculated and the measured conversions at 775 K for pressures of 1.0 and 1.8 bar,

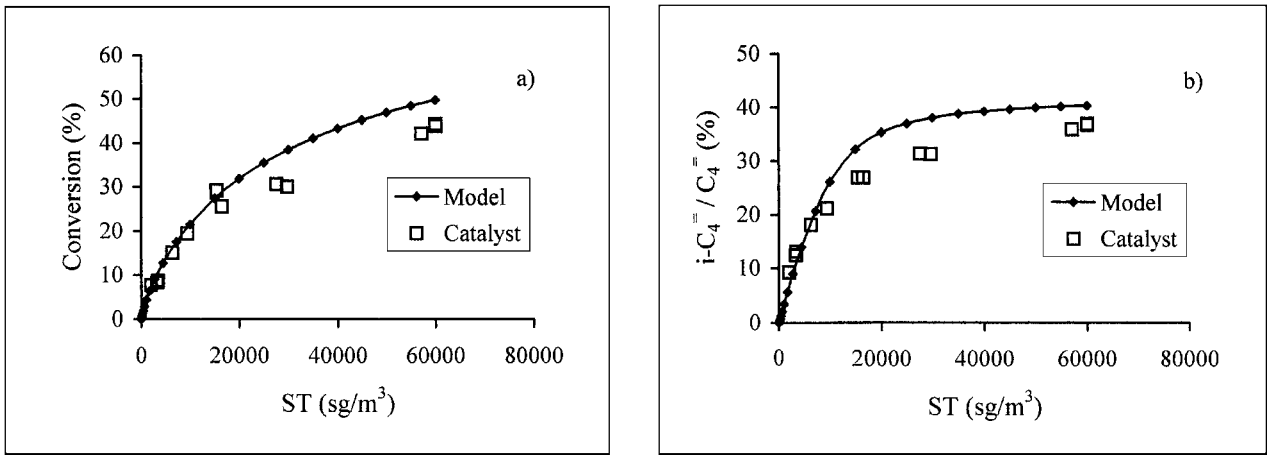

FIG. 8. Comparison of experimental data with the refined kinetic model. Experimental data: 0.1% Pt–ZSM5(480), 830 K, 1.8 bar, 10% *n*-butane, 20% H_2, 100 min on stream. Model parameters: $k_1 = 5.5 \times 10^{-5}$ m^3/s g, $k_2 = 8 \times 10^{-5}$ m^3/s g, $RTK_{C_4H_8} = 10$ bar^{-1}, $RTK_{C_4H_6} = 400$ bar^{-1}, $K_1 = 0.94$, $K_2 = 0.71$, $[C_4H_6]/[C_4H_8] = 0.027$.

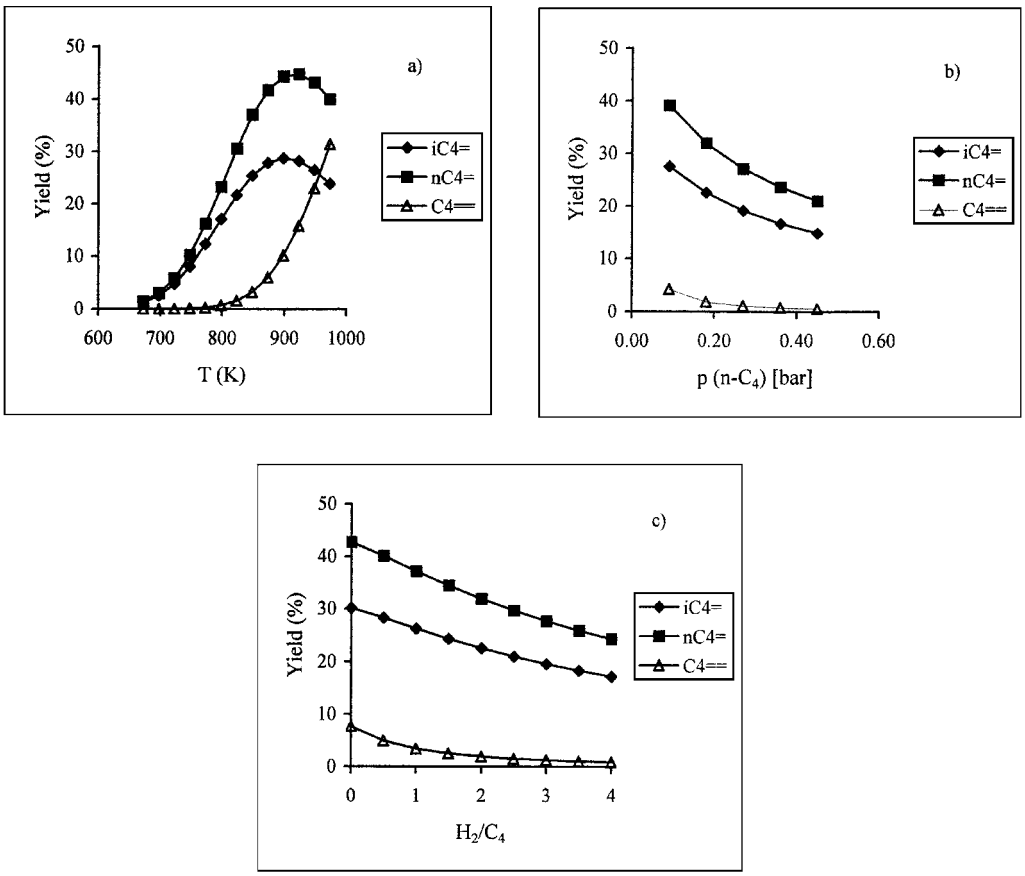

FIG. 9. (a) Dehydrogenation equilibrium as a function of temperature. Conditions: 1.8 bar, 10% *n*-butane, 20% H_2, 70% N_2. (b) Dehydrogenation equilibrium as a function of butane partial pressure. Conditions: 1.8 bar, H_2/*n*-butane = 2,830 K. (c) Dehydrogenation equilibrium as a function of H_2/*n*-butane. Conditions: 1.8 bar, 10% *n*-butane, 830 K.

with 0.5% Pt–ZSM5(480) as a catalyst. In model and experiment the conversion at high space times *decreased* with *increasing* pressure. This decrease was mainly caused by the less favorable thermodynamics at the higher pressure. At 1.8 bar thermodynamic equilibrium does not allow conversions higher than 32%. Due to side reactions the actual conversion can be higher. But since most of the side reactions are secondary reactions of butenes (6), the overall conversion is still very much governed by the dehydrogenation rate and, thus, subjected to thermodynamic constraints.

TABLE 7

Steady-State Yields of Butadiene (in mol% Carbon) and Deactivation Rates of Dehydrogenation and Isomerization as a Function of Temperature

	Temp (K)	Yield $C_4^{==}$ (%)	dk_1/dt (10^{-9} m^3 s^{-2} g^{-1})	dk_2/dt (10^{-9} m^3 s^{-2} g^{-1})
0.1% Pt	775	0.07	1.1	−0.08
	830	0.18	1.5	−0.07
	850	0.28	1.7	0.45
0.5% Pt	775	0.09	0.7	−0.02
	800	0.18	0.9	0.18
	830	0.39	2.9	0.37
	850	0.54	3.3	0.47

Note. dk_1/dt and dk_2/dt were calculated from the decrease in k_1 (dehydrogenation) and k_2 (isomerization) between 50 and 150 min on stream. For calculation of k_1 and k_2 see Appendix 1.

Conditions: 1.8 bar, WHSV = 260 h^{-1}, 10% *n*-butane, 20% H_2, 0.1 and 0.5% Pt–ZSM5(480).

Figure 11a shows how the apparent reaction rate ($r = [n\text{-}C_4H_{10}]x/ST$, x = conversion) depends on conversion, in the picture of the kinetic model. Initially (at zero conversion), the apparent reaction rate is higher at 1.8 bar than at 1.0 bar, because the reaction is first order in *n*-butane. With increasing conversion the fraction of free metal sites decreases and the contribution of the backward reaction increases (see Eq. [7]). Both effects are more pronounced at higher pressures. As a result, the apparent reaction rate at 1.8 bar becomes lower than that at 1.0 bar above a certain level of conversion (see Fig. 11a). Figure 11a also shows that the apparent reaction rate depends strongly on the conversion, which makes the extrapolation of initial reaction rates (at zero conversion) from the experimental data extremely difficult. The contribution of the backward reaction to this decrease of the apparent rate, i.e., the contribution of the term $1\text{-}[C_4H_8][H_2]/(K_{eq}[n\text{-}C_4H_{10}])$ in Eq. [7], can be corrected for by calculating the pseudo-first-order

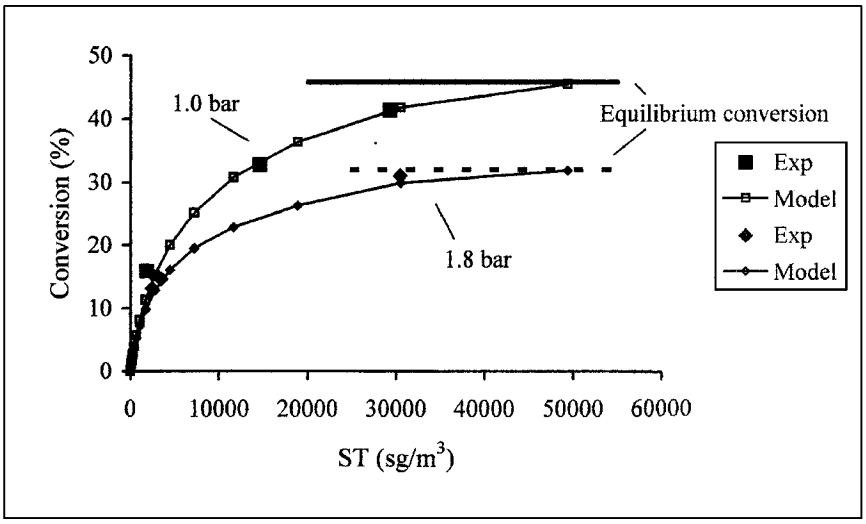

FIG. 10. Comparison of experimental data (solid symbols) with the refined kinetic model (open symbols). Experimental data: 0.5% Pt–ZSM5(480), 775 K, 10% *n*-butane, 20% H_2, 100 min time on stream. Model parameters: $k_1 = 1.4 \times 10^{-4}$ m^3/s g (estimated from Table 4), $k_2 = 5 \times 10^{-5}$ m^3/s g (measured for butene isomerization under these conditions), $RTK_{C_4H_8} = 20$ bar^{-1}, $RTK_{C_4H_6} = 1600$ bar^{-1}. Squares: 1.0 bar. Diamonds: 1.8 bar.

rate constant k_1, according to the method described in Appendix 1. The remaining decrease of k_1 with conversion (see Fig. 11b) is caused by the inhibiting effect of butene and butadiene sorption on the metal.

Due to the strong dependence of the rate and of the calculated rate constant k_1 on conversion, the reported rate data have to be interpreted very cautiously, i.e., more in terms of trends than in terms of absolute values. Moreover, it is emphasized that we do not see the kinetic model as a proof for the proposed reaction mechanism. It only serves as a tool to describe the effects of pressure and thermodynamics, under the assumption that the proposed reaction mechanism is correct.

Summarizing the effects discussed above, it can be stated that increasing pressures increase the intrinsic reaction rate. At higher conversions (above ~50% of the equilibrium conversion) this is overcompensated by the thermodynamic constraints and the inhibiting effect of product adsorption. The selectivity to oligomerization/cracking of butenes and to the formation of isobutane (via hydrogenation of isobutene) increased upon increasing the pressure. Thus, the overall conclusion is that high pressures are not favorable for the dehydroisomerization reaction.

Effect of Hydrogen to Hydrocarbon Ratio

The effect of the H_2/*n*-butane ratio was similar to the effect of pressure. It increases the activity at low conversions, but it also decreases the thermodynamically possible yield of butene (see Fig. 9c). At high conversions these two

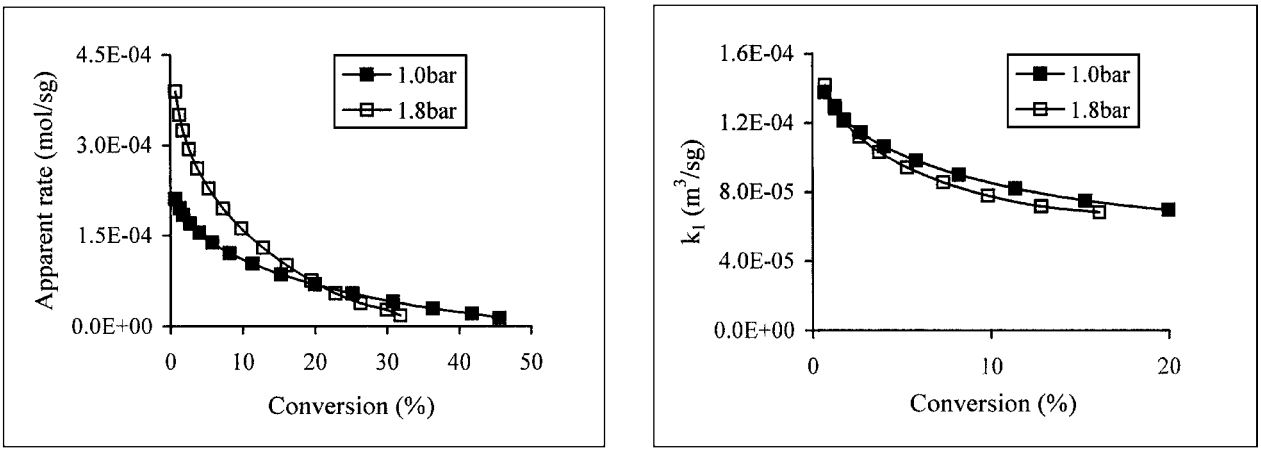

FIG. 11. Apparent reaction rate and pseudo-first-order rate constant of dehydrogenation, as calculated for the model. Model parameters: $k_1 = 1.4 \times 10^{-4}$ m^3/s g, $k_2 = 5 \times 10^{-5}$ m^3/s g, $RTK_{C_4H_8} = 20$ bar^{-1}, $RTK_{C_4H_6} = 1600$ bar^{-1}. Open symbols: 1.8 bar. Full symbols: 1.0 bar.

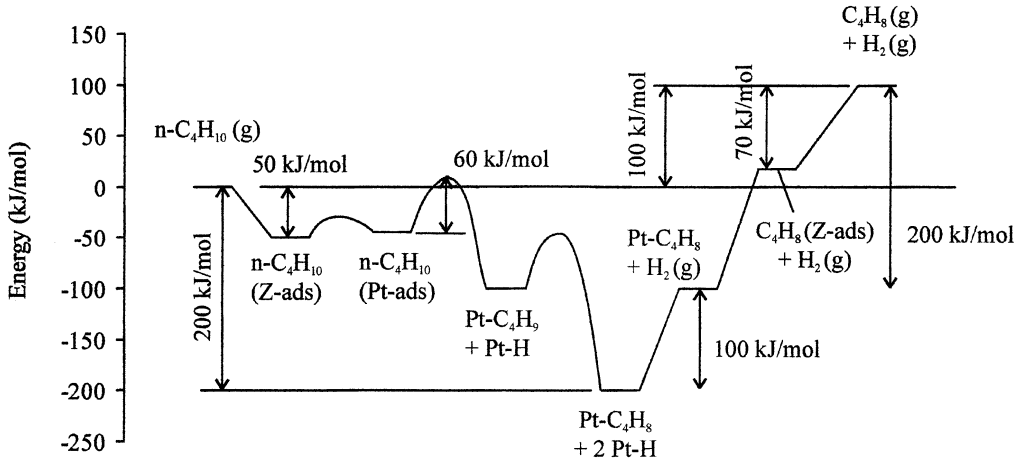

FIG. 12. Energy scheme of *n*-butane dehydrogenation in Pt–ZSM5. The activation energies and heats of sorption were estimated from literature values (see Appendix 3 for details).

factors nearly compensate each other (see Table 6). More important is, however, the influence of the H_2/*n*-butane ratio upon the selectivity to hydrogenolysis and the stability of the catalyst. The rate of methane formation depended linearly on the hydrogen partial pressure (Fig. 5). This indicates that methane is almost exclusively formed by hydrogenolysis and that the contribution of protolytic cracking of *n*-butane on the acid sites to the methane formation is only small (see the discussion of routes of by-product formation in Ref. 6). The selectivity to the hydrogenolysis products methane and ethane (ethane can also be formed by hydrogenation of ethene) increased drastically when the H_2/*n*-butane ratio was raised from 2.0 to 3.6, whereas the stability of the catalyst was not significantly improved. Therefore, we conclude that a H_2/*n*-butane ratio of 2 is a good compromise between selectivity and stability.

The positive order in hydrogen is at variance with the results of kinetic studies of dehydrogenation over Pt–Al_2O_3 (12, 16, 17, 22) and Pt–Au alloys (23) where a negative order of hydrogen (−0.5) was reported. This could be due to the fact that higher hydrogen/hydrocarbon ratios and lower temperatures were used in these studies, leading to a higher surface coverage of H_2, which inhibits the reaction (16). However, even in the absence of such an inhibiting effect, the order in hydrogen should not be larger than zero. The positive effect of hydrogen on the reaction rate (at low conversions) that we observed could be related to reduced butadiene formation. The yield of butadiene decreased from 0.17% to 0.10% to 0.07% with increasing H_2/*n*-butane ratios. We calculated the apparent order in hydrogen from the kinetic model. An order of 0.25 in hydrogen was obtained for $RTK_{C_4H_6} = 1600$ bar^{-1}. The order in hydrogen increased almost linearly with the value of $K_{C_4H_6}$. These results of the model calculation support the idea that the positive order in hydrogen could be indirectly caused by a reduced butadiene formation.

The Apparent Activation Energy

According to the rate equation, the activation energy should be the sum of the true energy of activation of step [i], i.e., the dissociation of *n*-butane, and a term describing the temperature dependence of the fraction of free metal sites (Θ_*).

Using transition-state theory, Cortright *et al.* obtained a true activation energy of 60 kJ/mol for step [i] (16), in line with surface science results (24). For the coverage term a simple expression cannot be given. Qualitatively, the activation energy should increase with the desorption energy of the metal-bonded hydrocarbon.

The zeolite can have a twofold effect on the activation energy. It increases the reactant concentration due to sorption in the pores. Moreover, the product alkene is desorbed from the metal not into the gas phase, but into the confined space of the zeolite pore. As a result, the desorption energy is reduced by the heat of sorption of the alkene in the zeolite pore, as shown in the energy scheme in Fig. 12.

Both above-mentioned factors reduce the apparent activation energy and could be responsible for the different activation energies of 0.1 and 0.5% Pt–ZSM5(480) (25 and 40 kJ/mol, respectively). We speculate that 0.1% Pt–ZSM5(480) has a higher fraction of metal sites in the zeolite pores (HREM photographs show that the distribution of Pt is rather inhomogeneous in both samples), leading to a higher contribution of sorption effects and, thus, a lower apparent activation energy.

CONCLUSIONS

We have shown that a combination of kinetics, thermodynamics, and sorption is necessary to explain the catalytic

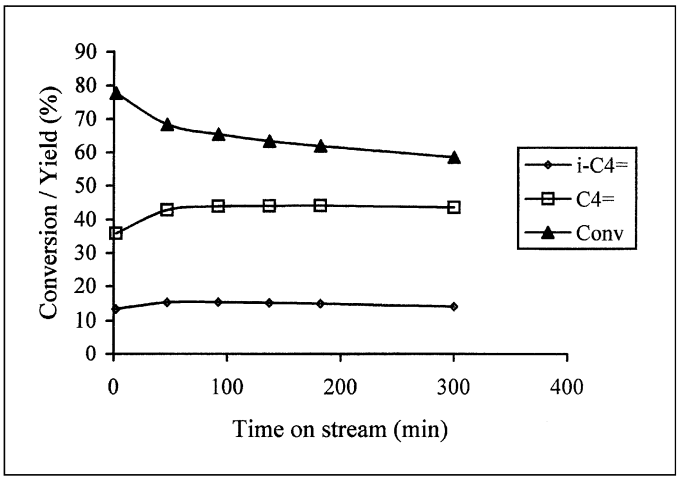

FIG. 13. Conversion of *n*-butane and yield of the sum of butenes and of isobutene. Conditions: 0.5% Pt–ZSM5(480), 830 K, 1 bar, 10% *n*-butane, 20% H_2, WHSV = 10 h^{-1}.

results of dehydroisomerization of *n*-butane. With respect to the optimization of the physical parameters temperature, pressure, and H_2/*n*-butane ratio, the following conclusions can be drawn. (i) High temperatures reduce the selectivity to by-products (oligomerization/cracking of butenes) and the thermodynamic constraints. However, above 830 K, these improvements are overcompensated by a loss in catalyst stability, which is attributed to poisoning by butadiene. (ii) Low pressures reduce the selectivity to by-products and the thermodynamic constraints. (iii) High H_2/*n*-butane ratios enhance unwanted hydrogenolysis reactions, while catalyst stability is not significantly improved. An optimum with respect to selectivity and stability was found for H_2/*n*-butane = 2.

These results and the results of Ref. (6) allow us to predict that the best yields of isobutene should be achieved at 830 K, 1 bar, with a H_2/*n*-butane ratio of 2, using 0.5% Pt–ZSM5(480) as a catalyst. In fact, a stable yield of 14–15% isobutene could be achieved under these conditions (see Fig. 13), which is one of the highest yields reported so far (see Table 8).

APPENDIX 1

Calculation of the Pseudo-First-Order Rate Constant of Dehydrogenation and Isomerization

The dehydrogenation of *n*-butane is an equilibrium reaction. Due to the backward reaction the observed reaction rate is lower than the intrinsic rate. In order to correct for this effect, a simple first-order kinetic model was assumed.

$$A \rightleftharpoons B \quad r = k_1[A] - k_{-1}[B]$$

r is given in mol/s g, k in m^3/s g, and the concentrations of A and B in mol/m^3. A represents *n*-butane, B the sum of linear butenes. The integration of this rate equation yields

$$k_1 = \frac{1}{ST}\frac{K}{1+K}\ln\left(1 - x - \frac{x}{K}\right) \qquad [10]$$

where $ST = m_{cat}/(dV_{total}/dt)$, x is conversion, and K is the equilibrium constant.

Equation [10] was used to calculate the pseudo-first-order rate constant of dehydrogenation (k_1) from the experimental conversions. Note that the model assumes that (i) the reaction order of *n*-butane is 1, and (ii) the order in hydrogen is zero and/or its concentration is constant and can be included in k_1. Only the overall equilibrium between *n*-butane and *n*-butene is considered. In a rigorous mathematical treatment, the three equilibria with the three linear butenes should be calculated separately. But if we assume that the double bond isomerization is always equilibrated (which is usually the case), the dehydrogenation reaction between can be described by a single equilibrium constant $K = ([cis\text{-2-butene}]_{eq} + [trans\text{-2-butene}]_{eq} + [1\text{-butene}]_{eq})/[n\text{-butane}]_{eq}$.

The formation of isobutene is not taken into account since it does not take place on the metal sites. As a consequence, the correction can only be used at low conversions, i.e., at low values of $[i\text{-}C_4^=]/\sum[C_4^=]$. Regarding the definition of the conversion x, we decided to use the total conversion of *n*-butane to all products instead of the conversion to butenes only. The reasoning behind this was that

TABLE 8

Patents for Dehydroisomerization of *n*-Butane

Catalyst	Feed	Temp (K)	WHSV (h^{-1})	Conv (%)	TOS (h)	Yield i-$C_4^=$ (%)	Max. yield i-$C_4^=$ (%)[a]	Ref.
Pt–ZSM5	H_2/*n*-C_4/Ar = 2/1/7	830	10	59	5	14.1	31	this work
Pt/Re–[B]–ZSM11	H_2/*n*-C_4 = 0.8, 3% H_2O	840	12.5	40	21	10	21	25
Pt–AMS–1B	H_2/*n*-C_4/He = 0.79/1/1.79	813	8.2	38	?	10.9	23	26
Sn/In/Pt–SiO_2/γ-Al_2O_3 + Boralite B	H_2/*n*-C_4/N_2 = 1/1/2	825	2	58	?	14.6	25	27
Ga–zeolite L	*n*-C_4	823	?	55	?	~10	24	28

[a] As calculated from thermodynamics.

isobutene and most of the by-products were formed as secondary products from the linear butenes (6) and should, thus, be included in the conversion. It is clear that this approach will lead to erroneous results if the selectivity to by-products formed by other, parallel routes is high.

For the pseudo-first-order rate constant of butene isomerization (k_2), the same method was applied. Here x was set equal to the ratio of $[\text{i-C}_4^=]/\sum[\text{C}_4^=]$. K was calculated as $[\text{i-C}_4^=]_{eq}/\sum[n\text{-C}_4^=]_{eq}$, the equilibrium concentration of isobutene divided by the sum of the equilibrium concentrations of the linear butenes. As above, this assumes that the linear butenes are already in equilibrium. The side reaction oligomerization/cracking is not taken into account by the model. As a result, the correction can only be applied when the selectivity to oligomerization/cracking is low, i.e., at low values of $[\text{i-C}_4^=]/\sum[\text{C}_4^=]$ (see Ref. 6). The assumption of first-order kinetics is correct. It was confirmed by butene isomerization experiments at different partial pressures. This is crucial since butene is a secondary product and its partial pressure strongly depends on the total conversion.

APPENDIX 2

Choice of the Model Parameters

In the kinetic model used to describe dehydroisomerization there are four free parameters, i.e., k_1, k_2, $K_{C_4H_8}$, and $K_{C_4H_6}$. k_1 and k_2 mainly influence the initial slope of the curves at low space times, while $K_{C_4H_8}$ and $K_{C_4H_6}$ have more effect on the values at high space times. While in principle all four parameters were varied in order to obtain a good fit of the experimental data, we restricted ourselves by certain boundary conditions in order to maintain the consistency of the model. An estimation of k_1, for example, could be obtained from the dehydrogenation rate at low conversions. In order to obtain a good fit of the experimental data, the model parameter k_1 had to be chosen higher than this estimate. This was due to the effect of coverage on the experimentally determined values of k_1 (see Fig. 11).

Likewise, an estimate of k_2 could be obtained from independent butene isomerization experiments with the same zeolite. A good fit of $\text{i-C}_4^= / \sum \text{C}_4^=$ at low space times was, however, possible only when k_2 was chosen higher than the experimentally determined value. We speculate that the difference could be due to the bifunctional nature of the reaction. Butenes that are formed on metal clusters in the zeolite pores are formed in the direct vicinity of the acid sites and isomerization can take place without having to establish an adsorption/desorption equilibrium with the gas phase. Additional experiments would be necessary, however, to prove this theory.

For the adsorption constants $K_{C_4H_8}$ and $K_{C_4H_6}$ experimental estimates could not be obtained. We therefore tried to make reasonable choices. From 830 to 775 K we let $K_{C_4H_8}$ and $K_{C_4H_6}$ increase by a factor of 2 and 4, respectively, which corresponds to a heat of sorption of 70 and 135 kJ/mol. These are realistic values.

APPENDIX 3

The Energy Diagram of Dehydrogenation

The heat of sorption of *n*-butane in ZSM5(480) was estimated from the measurements of Eder *et al.* (29). They found a heat of sorption of 58 kJ/mol in H–ZSM5. The contribution of interaction with the acid sites to this value is about 10 kJ/mol. Since the ZSM5 we used had a very low concentration of acid sites and is a more silicalite-like material, we used a heat of sorption of 50 kJ/mol in the scheme. The heat of sorption of the product butenes in ZSM5 was assumed to be 10–20 kJ/mol higher than that for the butane (30), i.e., approximately 70 kJ/mol.

The energy of desorption of *n*-butane from Pt(111) was determined by thermal desorption spectroscopy to be about 45 kJ/mol (31, 32). This value was taken as an estimation of the energy difference between *n*-butane in the gas phase and *n*-butane adsorbed on Pt (the concentration of this species will be practically zero; it either reacts or desorbs).

The activation energy for the dissociation of adsorbed *n*-butane was estimated from the results of surface science studies (24) and kinetic modeling (16). The energy of the di-σ-adsorbed state was estimated from the heat of sorption of isobutane on Pt–SiO_2 (20) and the heat of sorption of *n*-butane on Pt–NaY (21), which were between 200 and 250 kJ/mol. Also the heats of sorption of hydrogen and of butene were taken from these references. Note that with these values the correct reaction enthalpy is obtained ($\Delta H_R \sim 100$ kJ/mol).

ACKNOWLEDGMENTS

This work was performed under the auspices of NIOK, the Netherlands Institute of Catalysis Research. IOP Katalyse (IKA 94023) is gratefully acknowledged for financial support, and M. J. G. Janssen, from Exxon Chemical International Inc., Basic Chemicals Technology Europe, for supplying the ZSM5 samples.

REFERENCES

1. Frame, R. R., Stine, L. O., Hammershaimb, H. U., and Muldoon, B. S., *Erdöl Erdgas Kohle* **114**(7–8), 385 (1998).
2. Obenaus, F., Droste, W., and Neumeister, J., *in* "Ullmann's encyclopedia of industrial chemistry" (W. Gerhartz, Y. St. Yamamoto, F. T. Campbell, R. Pfefferkorn, and J. F. Rounsaville, Eds.), 5th ed., Vol. A4, p. 483. VCH, Weinheim, 1985–1986.
3. Rhodes, A. K., *Oil Gas J.* **90**, 36 (1992).
4. Schütte, G. F., Brinkmeyer, F. M., and Dunn, R. O., *Chim. Oggi* **12**, 39 (1994).
5. Gregor, J. H., Bakas, S. T., and Ulowetz, M. A., *Proc. Annu. Conv.-Gas Process Assoc.* **71**, 230 (1992).
6. Pirngruber, G. D., Seshan, K., and Lercher, J. A., *J. Catal.* **186**, 188 (1999).

7. Houzvicka, J., Nienhuis, J. G., Hansildaar, S., and Ponec, V., *Appl. Catal. A* **165**, 443 (1997).
8. Englisch, M., Ph.D. Thesis, University of Twente, Enschede, The Netherlands, 1996.
9. Froment, G. F., and Bischoff, K. B., *in* "Chemical Reactor Analysis and Design," 2nd ed., pp. 125–160. Wiley, New York, 1990.
10. Rodiguin, N. M., and Rodiguina, E. N., *in* "Consecutive Chemical Reactions, Mathematical Analysis and Development." van Nostrand, Princeton, NJ, 1964.
11. Roine, A., *in* "HSC Chemistry." Outokumpu Research Oy, Pori, Finland.
12. Loc, L. K., Gaidai, N. A., Gudkov, B. S., Kostyukovskii, M. M., Kiperman, S. L., Podkletnova, N. M., Kogan, S. B., and Bursian, N. R., *Kinet. Catal.* **27**, 1190 (1986).
13. Buonomo, F., Sanfilippo, D., and Trifiro, T., *in* "Handbook of Heterogeneous Catalysis" (G. Ertl, H. Knözinger, and J. Weitkamp, Eds.), Vol. 5, p. 2140. VHC-Wiley, Weinheim, 1997.
14. Cortright, R. D., and Dumesic, J. A., *Appl. Catal.* **129**, 101 (1995).
15. Cortright, R. D., Bergene, E., Levin, P., Natal-Santiago, M., and Dumesic, J. A., *in* "Proceedings, 11th International Congress on Catalysis, Baltimore, 1996" (J. W. Hightower, W. N. Delgass, E. Iglesia, and A. T. Bell, Eds.), Vol. 101, p. 1185. Elsevier, Amsterdam, 1996.
16. Cortright, R. D., Levin, P. E., and Dumesic, J. A., *Ind. Eng. Chem. Res.* **37**, 1717 (1998).
17. Lok, L. K., Gaidai, N. A., Gudkov, B. S., Kiperman, S. L., and Kogan, S. B., *Kinet. Catal.* **17**, 1184 (1986).
18. Cremer, P. S., Su, X., Shen, Y. R., and Somorjai, G., *J. Chem. Soc., Faraday Trans.* **92**, 4717 (1996).
19. Shahid, G., and Sheppard, N., *Can. J. Chem.* **69**, 1812 (1991).
20. Natal-Santiago, M. A., Podkolzin, S. G., Cortright, R. D., and Dumesic, J. A., *Catal. Lett.* **45**, 155 (1997).
21. Meriaudeau, P., Auroux, A., and Viornery, C., *Catal. Lett.* **41**, 139 (1996).
22. Loc, L. C., Gaidai, N. A., Kiperman, S. L., and Thoang, H. S., *Kinet. Catal.* **34**, 451 (1993).
23. Biloen, P., Dautzenberg, F. M., and Sachtler, W. M. H., *J. Catal.* **50**, 77 (1977).
24. Campbell, Ch. T., Sun, Y.-K., and Weinberg, W. H., *Chem. Phys. Lett.* **179**, 53 (1991).
25. O'Young, Ch.-L., Browne, J. E., Matteo, J. F., Sawicki, R. A., and Hazen, J., U.S. Patent 5.198.597 (1993), assigned to Texaco Inc.
26. Sikkenga, D. L., Nevitt, Th. D., and Jerome, N. F., U.S. Patent 4.433.190 (1984), assigned to Standard Oil Co.
27. Bellussi, G., Giusti, A., and Zanibelli, L., U.S. Patent 5.275.995 (1994), assigned to Eniricerche S.p.A., Snamprogetti S.p.A.
28. Kolumbus, A. J., Telford, C. D., and Young, D., EP 42.252 (1981), assigned to British Petroleum Co. Ltd.
29. Eder, F., Stockenhuber, M., and Lercher, J. A., *J. Phys. Chem. B* **101**, 5414 (1998).
30. Harflinger, R., Hoppach, D., Quachik, U., and Quitsch, K., *Zeolites* **3**, 123 (1983).
31. Salmerson, M., and Somorjai, G. A., *J. Phys. Chem.* **85**, 3835 (1981).
32. Xu, Ch., Koel, B. E., and Paffett, M. T., *Langmuir* **10**, 166 (1994).